Title

Interactions between gut permeability and brain structure and function in health and irritable bowel syndrome.

Authors

Witt, Suzanne
Bednarska, Olga
Keita, Åsa
et al.

Publication Date

2019

DOI

10.1016/j.nicl.2018.11.012

Peer reviewed

NeuroImage: Clinical 21 (2019) 101602

Contents lists available at ScienceDirect

NeuroImage: Clinical

journal homepage: www.elsevier.com/locate/ynicl

Interactions between gut permeability and brain structure and function in health and irritable bowel syndrome

Suzanne T. Witt[a,*], Olga Bednarska[b,c,1], Åsa V. Keita[b,1], Adriane Icenhour[a,b], Michael P. Jones[d], Sigrid Elsenbruch[e], Johan D. Söderholm[b], Maria Engström[a,f], Emeran A. Mayer[g], Susanna Walter[a,b,c]

[a] Center for Medical Image Science and Visualization (CMIV), Linköping University/US, 581 85 Linköping, Sweden
[b] Department of Clinical and Experimental Medicine, Linköping University, 581 83 Linköping, Sweden
[c] Department of Gastroenterology, Linköping University Hospital, 581 85 Linköping, Sweden
[d] Department of Psychology, Macquarie University, NSW 2109, Australia
[e] Institute of Medical Psychology & Behavioral Immunobiology, Essen University Hospital, Hufelandstr. 55, 45122 Essen, Germany
[f] Department of Medical and Health Sciences (IMH), Linköping University, 581 83 Linköping, Sweden
[g] Department of Medicine, UCLA, 10833 Le Conte Ave, Los Angeles, CA 90095, United States of America

ARTICLE INFO

Keywords:
Irritable bowel syndrome
Gut epithelial permeability
Resting state fMRI
Brain-gut interactions
Default mode network
Coping skills

ABSTRACT

Changes in brain-gut interactions have been implicated in the pathophysiology of chronic visceral pain in irritable bowel syndrome (IBS). Different mechanisms of sensitization of visceral afferent pathways may contribute to the chronic visceral pain reports and associated brain changes that characterize IBS. They include increased gut permeability and gut associated immune system activation, and an imbalance in descending pain inhibitory and facilitatory mechanisms. In order to study the involvement of these mechanisms, correlations between gut epithelial permeability and live bacterial passage, and structural and functional brain connectivity were measured in women with moderate-to-severe IBS and healthy women. The relationships between gut permeability and functional and anatomical connectivity were significantly altered in IBS compared with the healthy women. IBS participants with lower epithelial permeability reported increased IBS symptoms, which was associated with increased functional and structural connectivity in endogenous pain facilitation regions. The findings suggest that relationships between gut permeability and the brain are significantly altered in IBS and suggest the existence of IBS subtypes based on these interactions.

1. Introduction

Altered brain-gut interactions have recently been implicated in a number of conditions, including Parkinson's disease (Mulak and Bonaz, 2015), autism spectrum disorders (Grenham et al., 2011), depression (Cryan and Dinan, 2012; Dinan and Cryan, 2013), and irritable bowel syndrome (IBS) (Mayer et al., 2015a; Mayer and Tillisch, 2011). IBS has been referred to as a disorder of altered brain gut interactions (Drossman and Chang, 2016) characterized by chronic visceral pain and altered bowel patterns. While the specific pathophysiological mechanisms underlying chronic visceral pain in IBS remain incompletely understood (Ossipov et al., 2014), evidence for alterations imbalance of endogenous pain facilitatory and inhibitory mechanisms (Tracey and Bushnell, 2009) has been suggested as a potential component. Involvement of increased intestinal permeability (Al-Chaer et al., 2000; Bushnell et al., 2013; Gebhart, 2004; Gold and Gebhart, 2010) resulting in gut immune system activation in this process has also been proposed to be involved in IBS pathophysiology.

The bidirectional interactions between the brain and the gut previously reported in preclinical studies are mediated by multiple communication channels, including spinal and vagal afferents, and the two branches of the autonomic nervous system (Cryan and Dinan, 2012; Mayer et al., 2006; Mayer et al., 2015b; Rhee et al., 2009). Afferent signaling from the gut to the central nervous system, stemming from changes in gut functioning, can modulate brain function and behavior, while feedback from the central nervous system can affect gut function. Even though in humans the evidence for such bidirectional brain gut interactions is more limited, some studies support the concept that

* Corresponding author at: BrainsCAN, Western Interdisciplinary Research Building, Room 3190, University of Western Ontario, London, ON N6A 3K7, Canada.
E-mail addresses: switt4@uwo.ca, stwittphd@gmail.com (S.T. Witt).
[1] Both authors contributed equally.

https://doi.org/10.1016/j.nicl.2018.11.012
Received 20 March 2018; Received in revised form 15 October 2018; Accepted 16 November 2018
Available online 17 November 2018

changes in gut functioning can affect mood, behavior, and brain function (Ahluwalia et al., 2014; Pinto-Sanchez et al., 2017; Tillisch et al., 2013).

It has been proposed that brain regions related to default mode (Babo-Rebelo et al., 2016; Hall et al., 2010; Hong et al., 2016; Liu et al., 2016), salience detection, emotional arousal, sensorimotor functions, and central autonomic processing are involved in the processing and response to visceral afferent signals (Mayer et al., 2015a). In particular, the default mode network (DMN) has been implicated in the tight coupling of brain regions engaged in self-related processing with those engaged in processing of visceral signals (Babo-Rebelo et al., 2016). Increased connectivity between the DMN with emotion- and pain-related brain regions has previously been demonstrated in IBS (Hall et al., 2010), supporting an important role of this network in altered brain-gut interactions.

In addition to specific alterations mentioned above in DMN functional connectivity in IBS, it has previously been reported that in response to both the anticipation and delivery of rectal distension stimuli IBS subjects have altered activation in brainstem regions involved in pain modulation, including the periaqueductal gray (PAG) and rostral ventral medulla (RVM) (Berman et al., 2008; Naliboff et al., 2001; Tillisch et al., 2011). The PAG plays a key role in descending pain inhibition (Behbehani, 1995; Sandkuhler, 1996; Stamford, 1995), while the RVM is the final relay in the descending control of pain. The RVM receives input from the PAG, rostral anterior cingulate cortex (rACC), and amygdala, and can both inhibit and facilitate pain, making it a key region involved in descending pain modulation (Gebhart, 2004; Ossipov et al., 2014). Increased signaling from the amygdala to RVM has been implicated in the development of central sensitization within the context of chronic pain (Qin et al., 2003a, 2003b; Qin et al., 2003c; Veinante et al., 2013), particularly in the absence of concomitant activity in medial prefrontal cortex (Neugebauer, 2015; Neugebauer et al., 2009).

Converging lines of evidence point towards alterations in gut epithelial permeability as an important mechanism in altered gut brain communication (Kelly et al., 2015), and such permeability changes are thought to play a key role in the development of central sensitization in IBS (Al-Chaer et al., 2000; Bushnell et al., 2013; Gebhart, 2004; Gold and Gebhart, 2010). Increased gut permeability has previously been implicated in the sensitization of viscerosensory pathways and in the development of chronic visceral hypersensitivity characteristic of IBS (Al-Chaer et al., 2000; Bushnell et al., 2013; Gebhart, 2004; Gold and Gebhart, 2010). However, evidence from human studies to demonstrate a possible role of gut epithelial permeability, and associated brain structure and function in the development of IBS symptoms is currently not available.

In the current study, we investigated, for the first time, the relationship between resting state brain function and in vitro measures of gut barrier function in healthy women and women with moderate to severe IBS. Specifically, we tested for relationships between transcellular permeability (assessed by live bacterial passage of *Salmonella typhimurium*) and paracellular permeability and resting state functional connectivity in the DMN. We hypothesized that in women with IBS, both increased paracellular and transcellular permeability are associated with increased functional connectivity between the DMN and brain regions that play key roles in emotion and endogenous pain modulation, including PAG, RVM, rACC, medial prefrontal cortex, and amygdala compared with healthy women. We further explored whether any IBS symptoms may be mediating factors in the resting state connectivity between the DMN and emotion and pain modulation related brain regions. Finally, to determine the relative stability of any observed changes in resting state DMN functional connectivity associated with changes in gut permeability, we explored the relationship between WM microstructure and gut permeability for both the healthy women and women with IBS.

2. Methods

2.1. Participants

Thirty-two women with moderate-to-severe IBS, mean age 32.6 years (range 19–55), meeting Rome III criteria (7 IBS-Diarrhea, 8 IBS-Constipation, 17 IBS-Mixed), were recruited from the Gastroenterology Department, University Hospital in Linköping. IBS subjects reported having IBS-related symptoms for a median of 8 years (range: 1 year - 'whole life'). Fifteen healthy age-matched women, mean age 29.8 years (range 21–48), without medical history of gastrointestinal symptoms or complaints were recruited by advertisement as a control group (HCs). There was a non-significant difference in age between the two groups ($t_{45} = 0.93$; $p < 0.36$).

2.2. Study exclusion criteria

Exclusion criteria for both study groups were any organic gastrointestinal disease, metabolic or neurological disorders, and severe psychiatric disease (e.g., schizophrenia, bi-polar disorder, psychosis, etc.), as well as factors known to affect gut barrier function, including self-reported allergy, self-reported nicotine intake within the previous two months, and self-reported regular NSAID use. All participants were required to be fluent in Swedish.

2.3. Study Approval

Participants gave written, informed consent in accordance with the Helsinki Declaration. Approval for the study was granted by the Regional Ethical Review Board in Linköping, Sweden (Dnrs. 2013/506–32; 2014/264–32).

2.4. Study protocol

Participants first underwent MR scanning, then had biopsy samples taken via sigmoidoscopy within two weeks of the MR scan. All but three IBS participants met the scheduling requirements for having the biopsy within two weeks after the MR scan (IBS: mean 9 days (1–24); HCs: mean 6 days (1–14)). While the study protocol was designed for a maximum interval between MR scan and sigmoidoscopy of two weeks, failing to meet this requirement was not an exclusion criterion. It is generally accepted that intra-individual intestinal permeability measurements are quite stable over time, with at least three studies observing only minute intra-individual changes in permeability on repeated measures up to eight weeks apart (Mahmood et al., 2007; van Wijck et al., 2013; Zhou et al., 2018). Thus, we chose to include all participants who completed both the MR scanning and the sigmoidoscopy. However, to control for any potential effects of this time interval, the interval between MR scan and sigmoidoscopy was included as a covariate of no-interest for all subjects in all correlative analyses (as described in Section 2.11.3).

Prior to the MR scan, all participants were requested to fast for at least four hours (water was acceptable), refrain from taking any IBS-related, pain, or sleep medications for at least 24 h, refrain from consuming alcohol for at least 24 h, and refrain from any sort of bowel preparation for at least 24 h. We note that four IBS participants reported taking histaminergic sleep medications on an as needed basis, however, all self-reported refraining from taking any sleep medications for at least 48 h prior to MR scanning. All participants also underwent a standard MR screening to ensure no contraindications for MR scanning (e.g., metallic or electrical implants, history of claustrophobia, etc.). All participants included in the analyses in the current study were able to meet all inclusion criteria and pre-MRI scan requirements.

2.5. Self-report questionnaires

2.5.1. Screening questionnaires acquired for all participants

The Hospital Anxiety and Depression Scale (HADS) was used as a screening tool for symptoms of anxiety and depression (Zigmond and Snaith, 1983). Sum scores ranging from 0 to 21 indicate levels of anxiety and depression, respectively.

The Patient Health Questionnaire (PHQ-15) was implemented to assess the degree of somatization across fifteen different symptoms (Kroenke et al., 2002). Sum scores ranging from 0 to 30 indicate levels of symptom severity.

2.5.2. Questionnaires acquired for IBS participants

Gastrointestinal (GI) symptom severity was assessed with the IBS Severity Scoring System (IBS-SSS; Francis et al., 1997), evaluating the severity of abdominal pain, distension, stool frequency, consistency and interference with daily life. Sum scores define mild (75–175), moderate (175–300) and severe cases of IBS (scores > 300).

The Visceral Sensitivity Index (VSI) was used to evaluate GI symptom-specific anxiety in terms of cognitive, emotional and behavioral responses (Labus et al., 2004). Sum scores range from 0 to 75 with higher scores indicating more severe GI-specific anxiety.

The Coping Strategy Questionnaire (CSQ) was used to assess cognitive and behavioral strategies to cope with pain (Rosenstiel and Keefe, 1983), involving six subscales for cognitive strategies (ignoring pain, reinterpretation of pain, diverting attention, coping self-statements, catastrophizing, praying/hoping) and two subscales for behavioral strategies (increasing activity, increasing pain behavior). Sum scores between 0 and 36 for each subscale indicate how frequently a coping strategy is used. As we were interested primarily in IBS symptomology, we considered those subscales that correlated with IBS-SSS scores with a Spearman's rho > ± 0.3. This resulted in only the diverting attention (CSQ-Divert Attention), catastrophizing (CSQ-Catastrophizing), and increased pain behavior (CSQ-Pain Behavior) subscales being used for all subsequent analyses.

2.6. Magnetic resonance imaging

All MR images were acquired using a 32-channel head coil on a 3 T Philips Ingenia (Philips Healthcare, Best, The Netherlands) located at the Center for Medical Image Science and Visualization (CMIV) at Linköping University, Sweden. Ten minutes of eyes-closed RS-fMRI data were acquired with a single-shot, gradient-echo EPI sequence (TR/TE = 2000/37 ms; voxel = 3.59 × 3.59 × 4 mm^3; 28 slices; SENSE factor: 2) that effectively covered the whole brain. Diffusion weighted images were acquired using a 64-direction sequence (TR/TE = 9339/82 ms; voxel = 2 mm^3; b = 1000). T1-weighted images were acquired for all participants to ensure that they were otherwise free from any obvious pathologic abnormalities.

2.7. Sigmoidoscopy

Flexible sigmoidoscopies were performed by two experienced gastroenterologists (OB, SW) on all participants. Participants were required to fast for eight hours prior to the procedure and perform a colon preparation with an enema early the same morning. The procedure was performed without sedation with scope insertion approximately 30–40 cm ascending from linea dentata. Colonic biopsies were taken with biopsy forceps without a central lance and put directly in ice-cold, oxygenated Krebs buffer (115 mM NaCl, 1.25 mM $CaCl_2$, 1.2 mM $MgCl_2$, 2 mM KH_2PO_4, and 25 mM $NaHCO_3$, pH 7.35).

2.8. Epithelial permeability measurements

Complete methods regarding epithelial permeability experiments have been more fully described in our previous study on these same participants (Bednarska et al., 2017). Briefly, colonic biopsies were mounted in modified Ussing chambers (Harvard Apparatus Inc., Holliston, MA, USA) (Grass and Sweetana, 1988) as previously described (Keita et al., 2006). After 40 min of equilibration in Krebs buffer, 34 μCi/mL of the inert paracellular probe ^{51}Chromium (Cr)-EDTA (Perkin Elmer, Boston, MA, USA) and 10^8 CFU/mL live, green fluorescent protein (GFP)-labelled *Salmonella typhimurium*, prepared as previously described (Keita et al., 2006), were added to the mucosal side of each chamber. Serosal samples were collected at 0, 60 and 120 min and replaced with an equal volume of Krebs buffer. Live bacterial passage of *Salmonella typhimurium* (transcellular permeability) was determined at 488 nm in VICTOR™ *X3* multileader plate reader (Perkin Elmer, Sweden). ^{51}Cr-EDTA permeability was measured by gamma-counting (1282 Compugamma, Sweden), calculated during the 60–120 min period and presented as P_{app} (apparent permeability coefficient; cm/s $x10^{-6}$). The transepithelial potential difference (PD), short-circuit current (I_{sc}) and the transepithelial resistance (TER) across the tissues were monitored throughout the experiments to ensure tissue viability.

2.9. RS-fMRI analysis

The RS-fMRI images were reconstructed on the scanner and preprocessed according to the guidelines laid out for the GIFT group independent component analysis (ICA) toolbox (Allen et al., 2011). To briefly summarize, using SPM8 (http://www.fil.ion.ucl.ac.uk/spm) each participant's data were realigned using the INRIAlign tool (Freire and Mangin, 2001; Freire et al., 2002), spatially normalized into Montreal Neurologic Institute (MNI) space, and smoothed with an 8 mm FWHM Gaussian kernel. Each participant's translation and rotation correction parameters were individually examined to ensure that no participant had significant head motion larger than one voxel in any direction. No participants were excluded for excessive head motion. Spatial normalization into MNI space was initially performed on the mean functional volume for each participant using the standard procedures in SPM8. The calculated normalization parameters were then applied to each functional image set, respectively. The results of the spatial normalization process were also examined for each participant prior to submission to spatial smoothing. Functional connectivity was calculated using the GIFT v4.0a toolbox (http://icatb.sourceforge.net; Calhoun et al., 2001). A single ICA was performed across all 47 participants using the Infomax algorithm (Bell and Sejnowski, 1995), with back reconstruction of single-subject spatial maps from the raw data (Erhardt et al., 2011). Forty-five independent components were estimated, as determined using minimum length description (MDL) criteria adjusted to account for correlated samples (Li et al., 2007). Stability of the independent components was assured using ICASSO (Himberg et al., 2004; Li et al., 2007) with 500 iterations. Spatial regression with a previously published template of the DMN (Smith et al., 2009) was used to identify the component that most strongly corresponded to the DMN (Fig. A.1). A between-group, voxel-wise two-sample *t*-test was performed on this DMN component to determine whether any IBS-related differences in resting state functional connectivity were present. No significant between-group differences were noted in the DMN itself.

2.10. Diffusion tensor image analysis

The diffusion-weighted data were reconstructed on the scanner and processed using standard procedures in the FSL software suite (https://fsl.fmrib.ox.ac.uk/fsl/fslwiki/FSL; Jenkinson et al., 2012; Smith et al., 2004; Woolrich et al., 2009). Eddy correction was performed by registering the diffusion-weighted images to a common non-diffusion-weighted image using a mutual information cost function as employed in the FLIRT toolbox (Greve and Fischl, 2009; Jenkinson et al., 2002; Jenkinson and Smith, 2001). The tensor was then estimated, and scalar fractional anisotropy (FA) images, as a measure of WM fiber organization/microstructure integrity reflecting features including axon

caliber, fiber density, and myelination, were created for each subject individually. Tract-based spatial statistics (TBSS; Smith et al., 2007) was used to spatially normalize the data to a common MNI template using the FNIRT toolbox (Andersson et al., 2008) and create group-level maps of FA. A mean FA image calculated from all 47 subjects was used to mask the single subject maps (FA > 0.2) to focus the analyses on white matter regions.

2.11. Statistical analysis

2.11.1. IBS Rome III subgroups

As we previously did not find any relation between the established Rome III IBS subtypes (IBS-C, IBS-D, and IBS-M) and either paracellular or transcellular permeability (results not shown, Bednarska et al., 2017), the IBS participants were considered as a single group for all statistical analyses. Specifically, for ^{51}Cr-EDTA, we calculated a Kruskal-Wallis H of 1.97 (asymptotic sig. < 0.37) and for salmonella, a Kruskal-Wallis H of 0.14 (asymptotic sig. < 0.93).

2.11.2. Questionnaire data

As not all measures passed the Shapiro-Wilk normality test, non-parametric statistical methods were used for all between-group comparisons and correlation analyses involving the screening and IBS-specific questionnaire data. Specifically, Mann-Whitney *U* tests were used to assess between group differences. Spearman's rho was used to estimate the correlations between the epithelial permeability and IBS questionnaire data. Significance was determined using False Discovery Rate (FDR) correction at a critical q < 0.05. While not all of the questionnaire data were normally distributed, results are presented as mean ± standard deviation for ease of interpretation and comparison with other published results. All statistical analyses on the behavioral data were performed in SPSS v24 (https://www.ibm.com/products/spss-statistics). Graphs were created using GraphPad Prism 7 (https://www.graphpad.com/scientific-software/prism).

2.11.3. Neuroimaging data

To test for IBS-related differences compared with HCs in the correlation of permeability and DMN functional connectivity and WM microstructure, individual between-group covariate analyses were performed again using permutation analyses as implemented in the PALM tool (https://fsl.fmrib.ox.ac.uk/fsl/fslwiki/PALM; Winkler et al., 2014) with 10,000 iterations on the RS-fMRI and DTI data, respectively. To determine the relationships between permeability and DMN functional connectivity and WM microstructure in each study group (IBS and HCs), separate within-group, whole-brain covariate analyses for the RS-fMRI and DTI data were performed using permutation analyses as implemented in the PALM tool (again with 10,000 iterations). To limit the within-group results to only those regions observed in the between-group results, the within-group results were masked with the between-group results thresholded at $p < 0.05$, Family Wise Error corrected for comparing across the whole brain. The HADS anxiety and depression sub-scores and the number of days between the MR scan and biopsy were included in all analyses (both between- and within-group) as covariates of no interest for all subjects to statistically control for their respective effects on the brain function and structure. Threshold Free Cluster Enhancement (TFCE; Smith and Nichols, 2009) was applied. Results from these analyses were considered significant at p < 0.05, Family Wise Error (FWE) corrected for comparing across the whole brain. All renderings were created using Mango (http://ric.uthscsa.edu/mango/; J.L. Lancaster and M.J. Martinez).

2.11.4. Path modeling

Path modeling was performed on the paracellular permeability data only, as no significant correlations between the IBS questionnaire data and transcellular permeability were noted. Results (described more fully below Section 3.4) from the correlation analyses between paracellular permeability and IBS clinical characteristics identified the IBS-SSS, VSI, and CSQ-Pain Behavior as being significantly correlated with paracellular permeability. The simple, total correlation between paracellular permeability and RVM functional connectivity was calculated using the Pearson correlation coefficient to confirm the findings from the whole-brain RS-fMRI covariate analysis. This association was then decomposed into components that were either direct from paracellular permeability to RVM or indirect via the IBS-SSS, VSI score, or CSQ-Pain Behavior using mediation analysis. The decomposition was achieved using path modeling, which included both the direct path between permeability and RVM connectivity, as well as the indirect paths via the three questionnaires listed above. Calculations were performed in Mplus (https://www.statmodel.com/). Due to the uncertainty about the multivariate Normal assumption required by the significance test, formal statistical inference employed a nonparametric bootstrap with 2000 replications. Direct and indirect path coefficients are reported in standardized form.

3. Results

3.1. Screening questionnaires

Compared with HCs, the IBS subjects had significantly higher scores for somatization (16.1 ± 3.5 vs. 4.3 ± 3.5, $p_{corrected} < 0.0001$), anxiety (11.1 ± 3.6 vs. 3.6 ± 2.9, $p_{corrected} < 0.0001$), and depression (6.4 ± 4.2 vs. 1.5 ± 1.8, $p_{corrected} < 0.0001$). A total of twelve IBS participants showed elevated anxiety scores on the HADS, while five IBS participants were found to have a clinically relevant depression score on the HADS.

3.2. Clinical characteristics of IBS subjects

IBS participants reported IBS-related symptoms in the moderate-to-severe range (343 ± 93.3), elevated GI-specific anxiety (43.5 ± 14.4), and increased use of maladaptive coping skills including catastrophizing (14.4 ± 8.7), maladaptive pain behavior (16.3 ± 6.4), and diverting attention (11.7 ± 6.12).

3.3. Epithelial permeability

As we previously reported (Bednarska et al., 2017), the IBS group showed increased paracellular permeability to ^{51}Cr-EDTA (1.1×10^{-6} cm/s vs. 0.8×10^{-6}, $p < 0.03$) and increased transcellular permeability as indexed by live bacterial passage of *Salmonella typhimurium* (1027 ± 495 vs. 332 ± 153, $p < 3.5 \times 10^{-6}$) compared to HCs.

The Ussing chamber experiments showed stable PD after equilibration in all biopsies. The active net ion transport, assessed as I_{sc}, was similar in biopsies from IBS and HCs (results shown in (Bednarska et al., 2017). As previously reported (and reiterated here), there was significantly decreased transepithelial resistance (TER) in biopsies from IBS compared to HCs when experiments were started ($22.4 \pm 4.6\,\Omega \times cm^2$ vs. 26.2 ± 5.8, $p < 0.05$). At 90 min from start, TER was still lower in IBS (20.9 ± 4.3) compared to HC (24.3 ± 5.9), however, it did not reach statistical significance ($p < 0.07$) (Bednarska et al., 2017). For both study groups, though, the TER was found to remain stable across the entirety of the experiment. Additionally, as previously reported (Bednarska et al., 2017), the addition of *Salmonella typhimurium* was not found to affect either the passage of ^{51}Cr-EDTA or the TER.

3.4. Epithelial permeability and IBS clinical characteristics

By correlating the permeability results obtained in the Ussing chamber experiments with the self-report questionnaire data from the IBS subjects, we observed that the paracellular permeability was

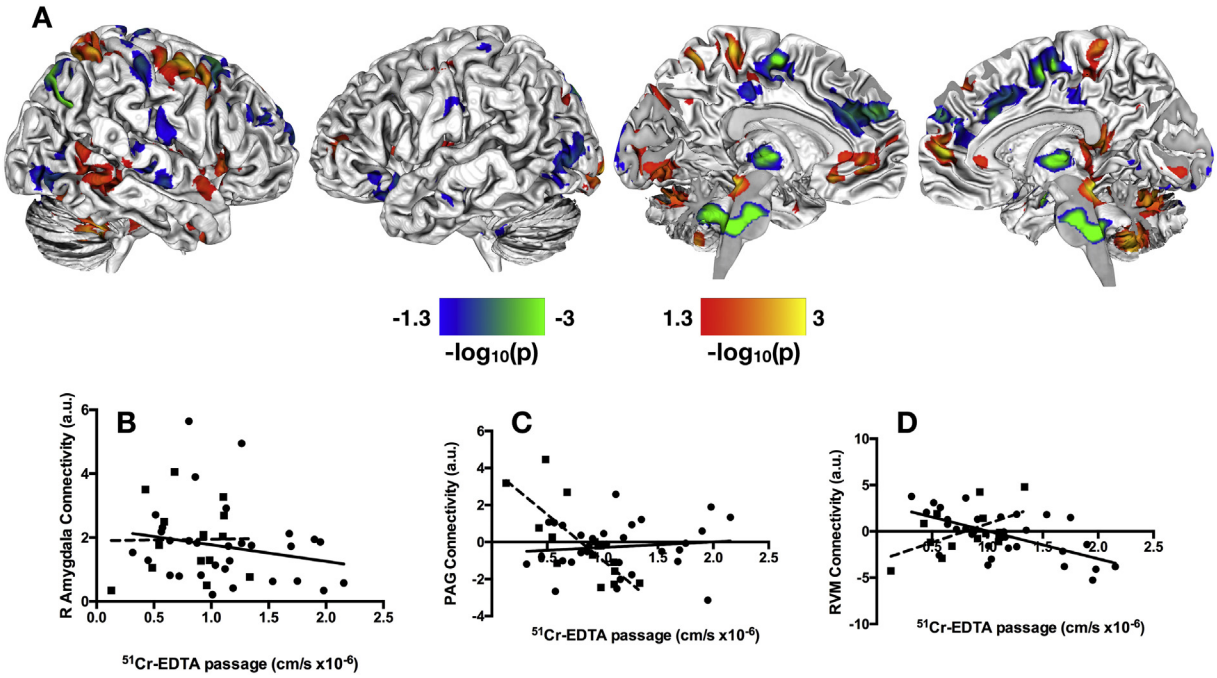

Fig. 1. Group differences in correlations between paracellular permeability and resting state functional connectivity in default mode network. A. Significant between-group differences in the correlation of paracellular permeability and resting state brain function in the DMN. **B.** Scatter plot with linear best-fit lines for the correlation between right amygdala connectivity and ^{51}Cr-EDTA passage for the IBS (circles, solid line) and HCs (squares, dashed line). **C.** Scatter plot with linear best-fit lines for the correlation between PAG connectivity and ^{51}Cr-EDTA passage for the IBS (circles, solid line) and HCs (squares, dashed line). **D.** Scatter plot with linear best-fit lines for the correlation between RVM resting state connectivity and ^{51}Cr-EDTA passage for the IBS (circles, solid line) and HCs (squares, dashed line). The statistical maps shown in **A** are thresholded at $p < 0.05$, Family Wise Error corrected for comparing across the whole brain. Color bars are scaled in terms of $-\log_{10}(p)$. Warm colors indicate brain regions with significant positive between-group differences for the (IBS-HCs) contrast; cool colors indicate brain regions with significant negative between-group differences for the (IBS-HCs) contrast.

negatively correlated with self-report scores from the IBS-SSS (Spearman's rho $= -0.41$, $p < 0.025$), VSI (Spearman's rho $= -0.42$, $p < 0.024$), and CSQ-Pain Behavior (Spearman's rho $= -0.502$, $p < 0.006$).

No significant correlations were observed between transcellular permeability and any of the questionnaire data.

3.5. Between-group differences of epithelial permeability and brain features

3.5.1. Paracellular epithelial permeability

3.5.1.1. Resting state DMN connectivity. We observed significant between-group differences in the correlation between paracellular epithelial permeability and resting-state brain connectivity in the DMN (Fig. 1A). In line with our hypothesis, we noted differences in DMN connectivity with sensorimotor regions, including bilateral pre−/postcentral gyri, thalamus, supplementary motor area (SMA), and paracentral lobule; emotion processing regions, including the right amygdala (Fig. 1B) and left orbital frontal cortex; cognitive processing regions, including bilateral middle and inferior frontal gyri; and pain processing regions, including the PAG (Fig. 1C) and RVM (Fig. 1D). This cluster within the RVM was localized by comparing its peak stereotactic coordinate with those previously reported in the literature (Bar et al., 2016; Napadow et al., 2009), as well as direct visual comparison with previously published structural and functional neuroimaging studies investigating the brainstem (Bianciardi et al., 2015; Son et al., 2014; Son et al., 2012).

From the within-group analyses masked with the between-group results, we observed that there was little overlap between the resting state brain features that correlated with paracellular permeability observed in the HCs with those in the IBS subjects, indicating significant IBS-related alterations. In general, HCs showed increased correlation between permeability and resting state brain function in a more diverse and distributed set of brain regions compared to the IBS subjects (Fig. 2A-B). We noted a few key differences, though. Most notably, increased functional connectivity of the right amygdala was correlated with decreasing permeability in IBS subjects, whereas no relationship between amygdala and permeability was found for the HCs (Fig. 1B). In HCs, decreased paracellular permeability was associated with increased connectivity between the DMN and PAG, while no such relationship between DMN and PAG was observed in the IBS subjects (Fig. 1C). There were also a few points of overlap between the brain features observed in HCs and those observed for IBS. The main region showing overlap between the HCs and the IBS subjects was found in the RVM (Fig. 1D). Within the RVM, HCs showed a positive correlation between brain connectivity with permeability, whereas the IBS subjects showed a negative correlation between these parameters.

3.5.1.2. White matter microstructural integrity (fractional anisotropy). We noted significant between-group differences in the correlation of epithelial permeability and FA across numerous major white matter tracts (Fig. 3A). Among the association fibers, between-group differences were found in bilateral cingulum bundles (both cingulate and hippocampal aspects), bilateral superior longitudinal and superior fronto-occipital fasciculi, and fornix. Among the commissural fibers, differences were observed in all aspects of the corpus callosum (genu, body, and splenium). Positive between-group differences, though, were most numerous in the projection fibers, including bilateral anterior, posterior, and superior corona radiata; anterior, posterior, and retrolenticular limbs of the internal capsule; cerebral peduncle; inferior, middle, and superior cerebellar peduncle; right medial lemniscus; right corticospinal tract; and bilateral posterior thalamic radiation. Negative between-group differences were observed in left anterior and posterior corona radiata, right superior corona radiata, right posterior thalamic radiation, right corticospinal tract, left superior

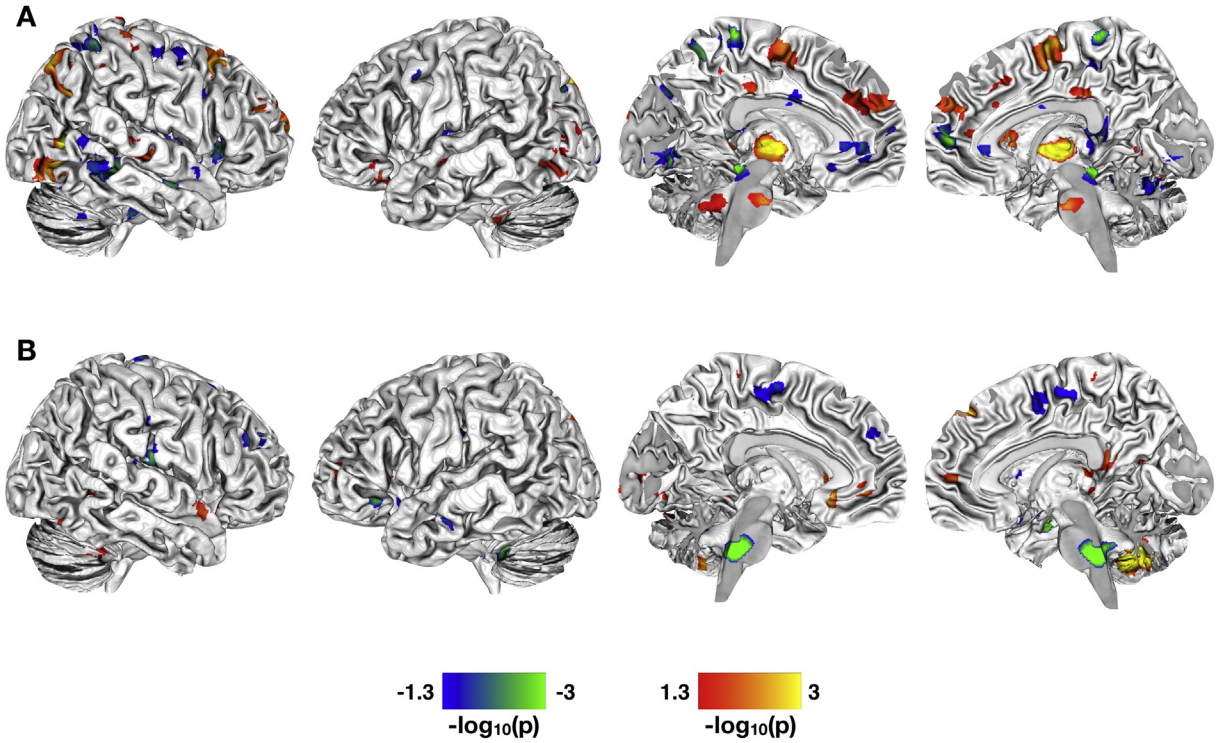

Fig. 2. Correlations between paracellular permeability and brain function in healthy controls and women with IBS. A. Significant whole-brain correlations between levels of ^{51}Cr-EDTA passage (paracellular permeability) and resting state brain function in the DMN for the HCs. **B.** Significant whole-brain correlations between levels of ^{51}Cr-EDTA passage and resting state brain function in the DMN for the IBS patients. All statistical maps are thresholded at $p < 0.05$, Family Wise Error corrected for comparing across the whole brain and masked with the significant group-difference results shown in Fig. 1A. Color bars are scaled in terms of $-\log_{10}(p)$. For the statistical maps shown, warm colors indicate brain regions with increased resting state functional connectivity with increased paracellular passage of ^{51}Cr-EDTA; cool colors indicate regions with increased functional connectivity with decreased paracellular passage of ^{51}Cr-EDTA.

longitudinal fasciculus, splenium of the corpus callosum, and middle cerebellar peduncle.

When examining the within-group results masked with the between-group results, we note that the HCs have increased FA with increased epithelial permeability in a number of association fibers including fornix and bilateral superior and inferior longitudinal fasciculi; commissural fibers including all aspects of the corpus callosum; and projection fibers including bilateral corona radiata, cerebral and cerebellar peduncles, corticospinal tracts, thalamic radiations, and internal and external capsules (Fig. 3B). Increased FA in relation to decreased epithelial permeability was observed in many of these same tracts for the IBS patients, specifically noting increased FA in relation to decreased epithelial permeability in the hippocampal aspect of the left cingulum bundle, the fornix cres, and numerous projection fibers including, bilateral corona radiata (anterior, posterior, and superior), cerebral and cerebellar peduncles, bilateral corticospinal tracts, bilateral thalamic radiations, and bilateral internal and external capsules (Fig. 3C). Only limited significant within-group clusters for increased FA in relation to decreased epithelial permeability were noted for the HCs. Similarly, only a few significant clusters for increased FA in relation to increased epithelial permeability were noted for the IBS participants.

3.5.2. Transcellular epithelial permeability

3.5.2.1. Resting state DMN connectivity. As with paracellular permeability, the between-group analysis on transcellular permeability revealed a number of brain regions exhibiting significant differences in the correlation of transcellular permeability with resting state connectivity of the DMN (Fig. 4A). We observed between-group differences in sensorimotor regions including bilateral pre−/postcentral gyri, SMA, and paracentral lobule; emotion processing regions including the anterior cingulate cortex, insula, and orbital frontal cortex; cognitive processing regions including middle and inferior frontal gyri; and pain processing regions including pons and RVM.

In contrast, the within-group results masked with the between-group results indicated more overlap between the changes in DMN connectivity observed for HCs with those observed for IBS compared with the epithelial permeability results. Within the regions observed in the between-group results, only limited group by permeability interactions were observed. The HCs exhibited increased correlation between transcellular permeability and RS functional connectivity between DMN and bilateral orbital frontal cortices; decreased correlation between transcellular permeability and RS functional connectivity between DMN and small clusters in ACC, pre−/postcentral gyri, middle frontal gyri, and RVM (Fig. 4B). In contrast, we observed increased correlation between transcellular permeability and DMN connectivity in small clusters in SMA, MFG, and pons in the IBS participants (Fig. 4C). The only region exhibiting decreased correlation between transcellular permeability and DMN functional connectivity in the IBS participants was in the left insula.

3.5.2.2. White matter microstructural integrity. We noted significant between-group differences in the correlation of transcellular permeability and FA across numerous major white matter tracts (Fig. 5A). For association fibers, between-group differences were found in bilateral cingulum bundles; bilateral superior longitudinal, superior fronto-occipital, and inferior longitudinal fasciculi; and fornix. Among the commissural fibers, differences were observed in all aspects of the corpus callosum (genu, body, and splenium). Positive between-group differences were again most numerous in the projection fibers, including bilateral anterior, posterior, and superior corona radiata; anterior, posterior, and retrolenticular limbs of the internal capsule; cerebral peduncle; inferior, middle, and superior cerebellar peduncle; right medial lemniscus; bilateral corticospinal tract; and bilateral

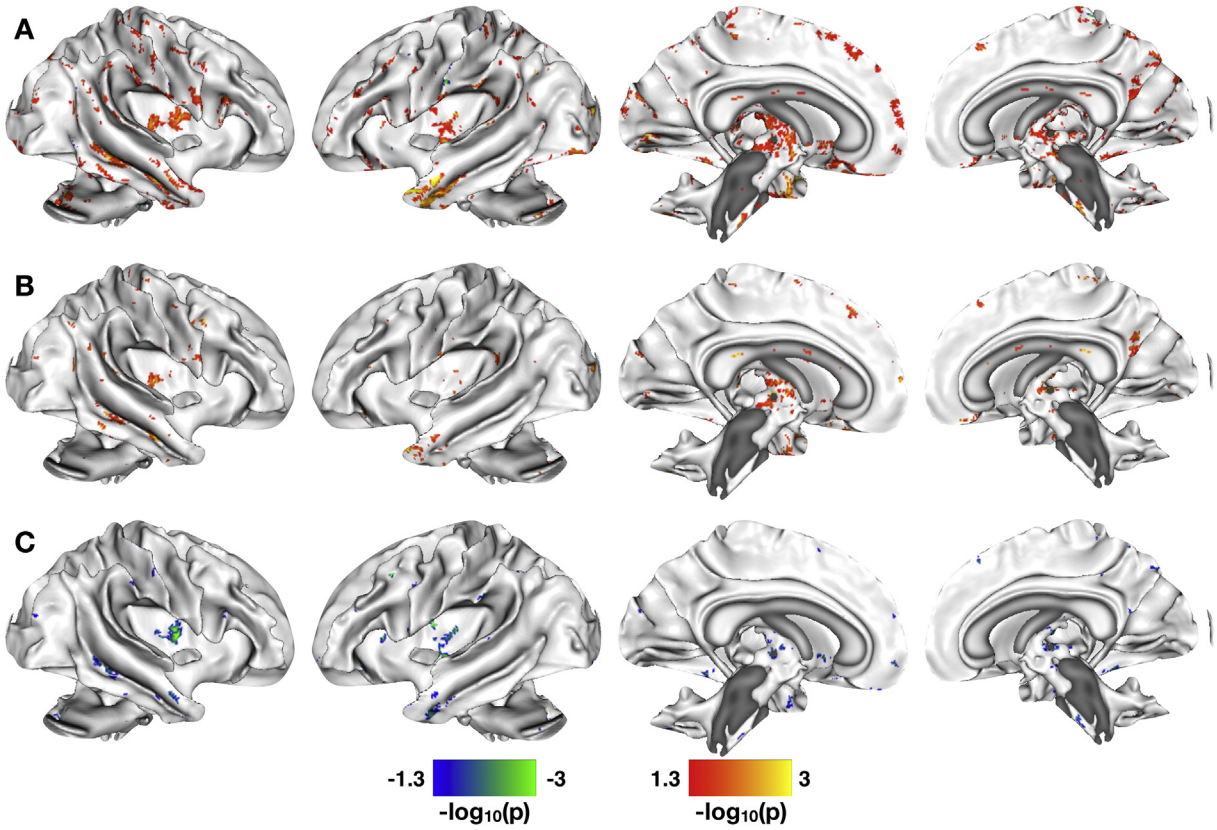

Fig. 3. Correlations between paracellular permeability and white matter microstructural integrity. A. Significant between-group differences in the correlation of paracellular permeability and fractional anisotropy (FA). **B.** Significant whole-brain correlations between levels of ^{51}Cr-EDTA passage and WM microstructure as quantified by FA for the HCs. **C.** Significant whole-brain correlations between levels of ^{51}Cr-EDTA passage and WM microstructure as quantified by FA for the IBS patients. All statistical maps are thresholded at $p < 0.05$, Family Wise Error corrected for comparing across the whole brain. Color bars are scaled in terms of $-\log_{10}(p)$. For the statistical maps shown in **A**, warm colors indicate WM tracts with significant positive between-group differences for the (IBS-HCs) contrast; cool colors indicate WM tracts with significant negative between-group differences for the (IBS-HCs) contrast. For the statistical maps shown in **B–C**, results are masked with significant group-differences shown in **A.** Warm colors indicate WM tracts with increased FA with increased paracellular passage of ^{51}Cr-EDTA; cool colors indicate tracts with increased FA with decreased paracellular passage of ^{51}Cr-EDTA.

posterior thalamic radiation. Negative between-group differences were observed in aspects of the cingulum bundles, including those in the region of the cingulate gyrus and hippocampus, the splenium of the corpus callosum, bilateral corona radiata (anterior, posterior, and superior), bilateral corticospinal tracts, left retrolenticular part of the internal capsule, and middle cerebellar peduncle.

Results from the within-group analyses masked with the between-group results indicated that the HCs were driving most of these between-group differences, with some key clusters of divergence observed in the IBS group. The HCs exhibited increased FA in relation to increased transcellular permeability in bilateral superior and inferior longitudinal fasciculi, the body and splenium of the corpus callosum, bilateral corona radiata, middle cerebellar peduncles, and right thalamic radiations (Fig. 5B). The IBS participants exhibited increased FA correlated with increased transcellular permeability in the left superior longitudinal fasciculus, the genu and splenium of the corpus callosum, the middle cerebellar pedunle, and the posterior thalamic radiation (Fig. 5C). One key area of divergence from the HCs exhibiting increased FA in relation to decreased transcellular permeability in the IBS group was noted in the right cingulum bundle (hippocampus). Increased FA in relation to decreased transcellular permeability was also observed in right anterior and posterior internal capsule and bilateral cerebral peduncles in the IBS participants.

3.5.3. Associations in gut permeability, RS connectivity, and IBS symptoms

To explore if the association between paracellular permeability and RS brain function is related to clinical and behavioral parameters in the IBS participants, a path analysis was performed (Fig. 6). We chose to model the direct effects of paracellular permeability on RVM resting state functional connectivity, given that nuclei in this region play an important role in endogenous pain modulation. In selecting relevant clinical and psychological symptoms to use for modeling indirect effects, we chose the three self-report questionnaires that correlated most strongly with levels of paracellular permeability. These were the IBS-SSS (Spearman's rho $= -0.41$, $p < 0.025$), VSI (Spearman's rho $= -0.42$, $p < 0.024$), and CSQ-Pain Behavior (Spearman's rho $= -0.502$, $p < 0.006$). The results of the path modeling indicated that there was a significant total effect of permeability on RVM connectivity (-0.603 ± 0.134, $p < 0.001$), identical to what we observed with the resting state DMN connectivity results (Fig. 1D). This total effect could be divided into a significant direct effect (-0.399 ± 0.174, $p < 0.022$) and a trend-level indirect effect (-0.204 ± 0.11, $p < 0.062$). The indirect effect was almost entirely driven by the CSQ-Pain Behavior sub-score (-0.203 ± 0.090, $p < 0.024$). The indirect effects of the IBS-SSS and VSI total score were non-significant ($p > 0.3$). These observations concerning the indirect effects suggest that the influence of paracellular permeability on RVM connectivity may be modulated by the degree to which the IBS subjects report engaging in maladaptive pain behaviors, rather than symptom severity or visceral specific anxiety.

4. Discussion

We observed statistically robust differences in the correlations

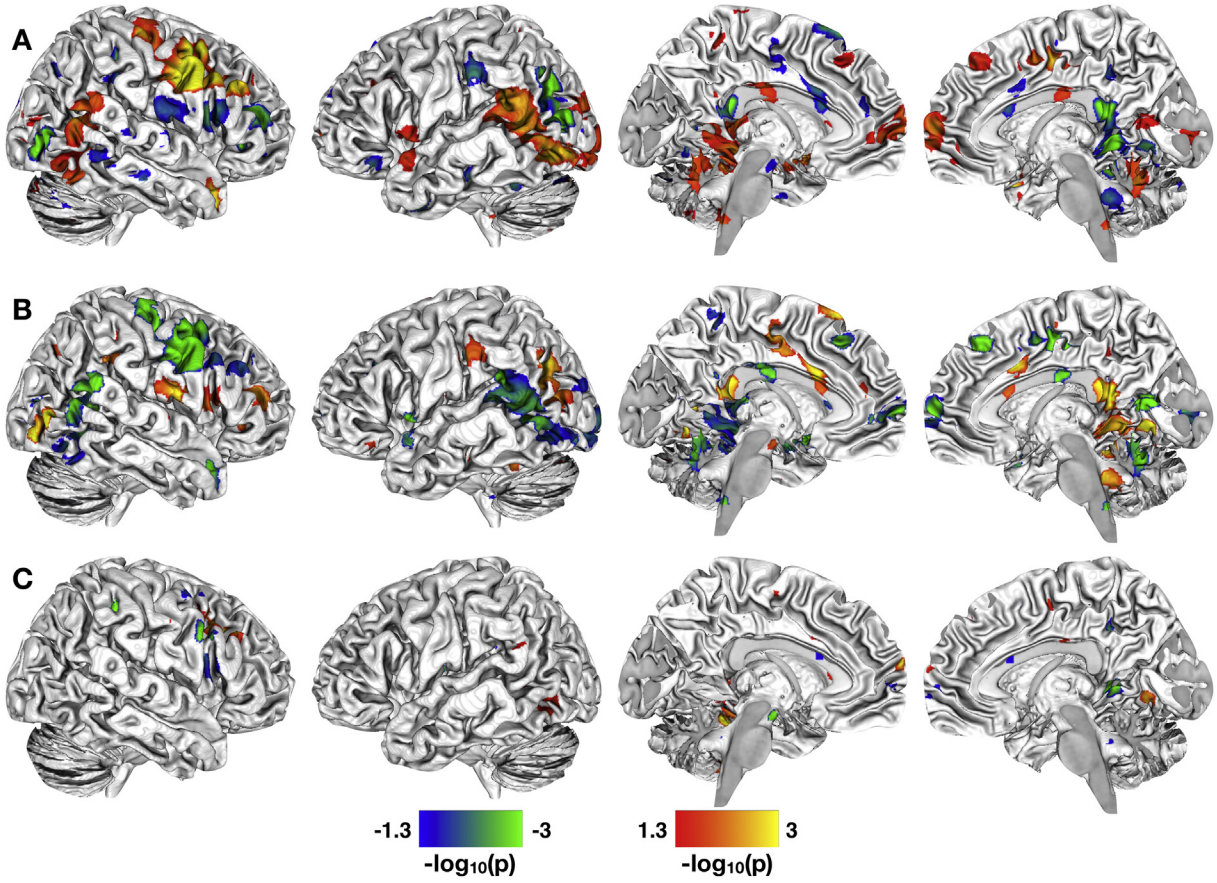

Fig. 4. Correlations between transcellular permeability and resting state functional connectivity in default mode network. A. Significant between-group differences in the correlation of transcellular permeability and resting state brain function in the DMN. **B.** Significant whole-brain correlations between levels of *Salmonella typhimurium* passage (transcellular permeability) and resting state brain function in the DMN for the HCs. **C.** Significant whole-brain correlations between levels of *Salmonella typhimurium* passage and resting state brain function in the DMN for the IBS patients. The statistical maps shown in **A** are thresholded at $p < 0.05$, Family Wise Error corrected for comparing across the whole brain. Color bars are scaled in terms of $-\log_{10}(p)$. Warm colors indicate brain regions/WM tracts with significant positive between-group differences for the (IBS-HCs) contrast; cool colors indicate brain regions/WM tracts with significant negative between-group differences for the (IBS-HCs) contrast. For the statistical maps shown in **B–C**, results are masked with significant group-differences shown in A. Warm colors indicate WM tracts with increased FA with increased transcellular passage of *Salmonella typhimurium*; cool colors indicate tracts with increased FA with decreased transcellular passage of *Salmonella typhimurium*.

between measures of paracellular and transcellular epithelial permeability and structural and functional brain features between women with moderate-to-severe IBS and healthy women. Functionally, these between-group differences were readily identifiable at rest and represented a distributed set of cortical, sub-cortical, cerebellar, and brainstem structures that corresponded with those previously linked to default mode, cognitive, sensorimotor, salience, central autonomic, pain, and emotional processing, as well as in many of the major white matter tracts connecting these regions. Functionally, these brain features were linked to resting-state activity within the DMN, providing the first direct evidence that changes in gut permeability may be tightly linked to the self-referential processing characteristic of the DMN. Structurally, the WM fiber organization among many of these regions was also enhanced, suggesting that the observed pattern of communication among these brain regions may reflect persistent regional alterations in brain function. Previous research in adults has demonstrated positive associations between WM microstructure and resting state functional connectivity of the DMN (van den Heuvel et al., 2008) and between the amygdala and ventromedial PFC and rACC (Jalbrzikowski et al., 2017), indicating a relationship between functional and structural connectivity at rest both within a canonical resting-state network and between specific brain regions.

4.1. Brain and gut permeability interactions in health

The associations between paracellular and transcellular permeability and brain structure/function were not identical, suggesting that both paracellular and transcellular permeability can independently affect brain features and should both be considered as potential facilitatory mechanisms for brain-gut interactions. In addition to confirming our hypothesis of the role of cognitive, default mode, sensorimotor, salience, emotion, and central autonomic processing regions would be associated with gut epithelial permeability, we also noted that increases and decreases in both paracellular and transcellular permeability were related to increased connectivity between the DMN and pain processing regions, particularly in the brainstem. Previous reviews of brain-gut interactions in functional gastrointestinal disorders, such as IBS, have focused on pain processing regions, such as PAG, primarily in relation to the brain's response to rectal distention and rectal hypersensitivity. That these pain-related brainstem regions (Fairhurst et al., 2007; Millan, 2002; Sandkuhler, 1996; Stamford, 1995) are apparent in healthy women with no reported history or complaints of chronic pain or gastrointestinal pain suggests that these regions may play a role in the normal processing of ascending visceral afferent signaling. Finally, given the key role changes in gut epithelial permeability play in facilitating brain-gut interactions, studies examining the effects of changes in gut function on brain function and structure in health and disease

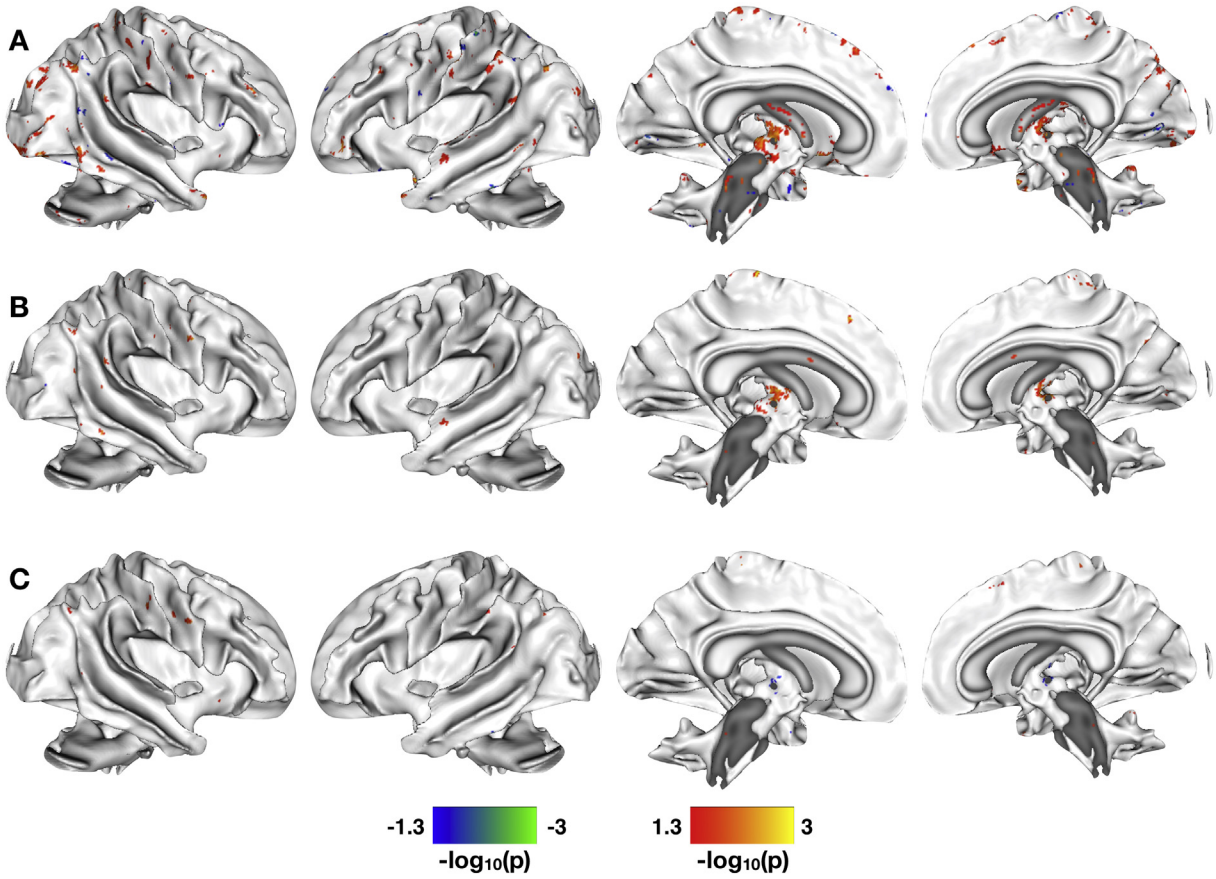

Fig. 5. Correlations between transcellular permeability and white matter microstructural integrity. A. Significant between-group differences in the correlation of transcellular permeability and fractional anisotropy (FA). **B.** Significant whole-brain correlations between levels of *Salmonella typhimurium* passage and WM microstructure as quantified by FA for the HCs. **C.** Significant whole-brain correlations between levels of *Salmonella typhimurium* passage and WM microstructure as quantified by FA for the IBS patients. All statistical maps are thresholded at $p < 0.05$, Family Wise Error corrected for comparing across the whole brain. Color bars are scaled in terms of $-\log_{10}(p)$. For the statistical maps shown in **A**, warm colors indicate WM tracts with significant positive between-group differences for the (IBS-HCs) contrast; cool colors indicate WM tracts with significant negative between-group differences for the (IBS-HCs) contrast. For the statistical maps shown in **B–C**, results are masked with significant group-differences shown in **A.** Warm colors indicate WM tracts with increased FA with increased transcellular passage of *Salmonella typhimurium*; cool colors indicate tracts with increased FA with decreased transcellular passage of *Salmonella typhimurium*.

may need to consider the role that gut epithelial permeability plays in brain function and structure.

4.2. Brain and gut permeability interactions in IBS

Contrary to our primary study hypothesis, IBS participants with lower levels of paracellular permeability exhibited increased resting state functional connectivity between the DMN and predominantly emotion and pain processing regions. The combination of functional connectivity among the right amygdala and RVM, in particular, would seem to suggest that these subjects, despite having no evidence for increased paracellular permeability, have a compromised endogenous pain inhibition system (Gebhart, 2004). We did not observe increased connectivity between the RVM and DMN for IBS participants with lower levels of live bacterial passage, suggesting perhaps that paracellular permeability may represent a more prevalent path to central sensitization than live bacterial passage. The increased connectivity between DMN and primarily cognitive and sensorimotor brain regions in relation to both increased paracellular permeability and live bacterial passage would suggest, though, that IBS participants with increased permeability may more effectively engage their endogenous pain inhibition systems. However, we note that no evidence for increased connectivity between DMN and PAG, a key descending pain inhibitory region, in the IBS group in association with either paracellular or transcellular permeability, suggesting that even IBS participants with elevated gut permeability may still exhibit some level of imbalance between the endogenous pain inhibitory and facilitatory mechanisms despite generally reporting fewer IBS-related symptoms. We further observed in the exploratory analyses relating gut permeability and WM microstructure that lower levels of permeability (both paracellular permeability and live bacterial passage) were associated with increased fiber organization in major tracts connecting the spinal cord and brainstem to the cortex and cerebellum, suggesting an increased reliance on these projection fibers that communicate ascending and descending signals from and to the spinal cord. While increased gut permeability was also associated with increased fiber organization in some of these same projection fibers, the pattern of results was much less extensive.

Ultimately, the differences in brain gut interactions in relation to levels of paracellular and transcellular permeability suggest that both top-down and bottom-up mechanisms are involved IBS pathophysiology. Particularly, for paracelluar permeability, the results suggest the existence of two potential new sub-groups of IBS patients, those with elevated paracellular permeability and those with more normal levels of paracellular permeability. For the IBS participants with elevated paracellular permeability, the brain may engage descending pain inhibition systems, responding to enhanced visceral signaling related to low-grade immune activation induced by increased paracellular passage. This is supported by our recently published observations from this same subject population, showing that mast cell degranulation was also negatively correlated with IBS-SSS (like paracellular permeability),

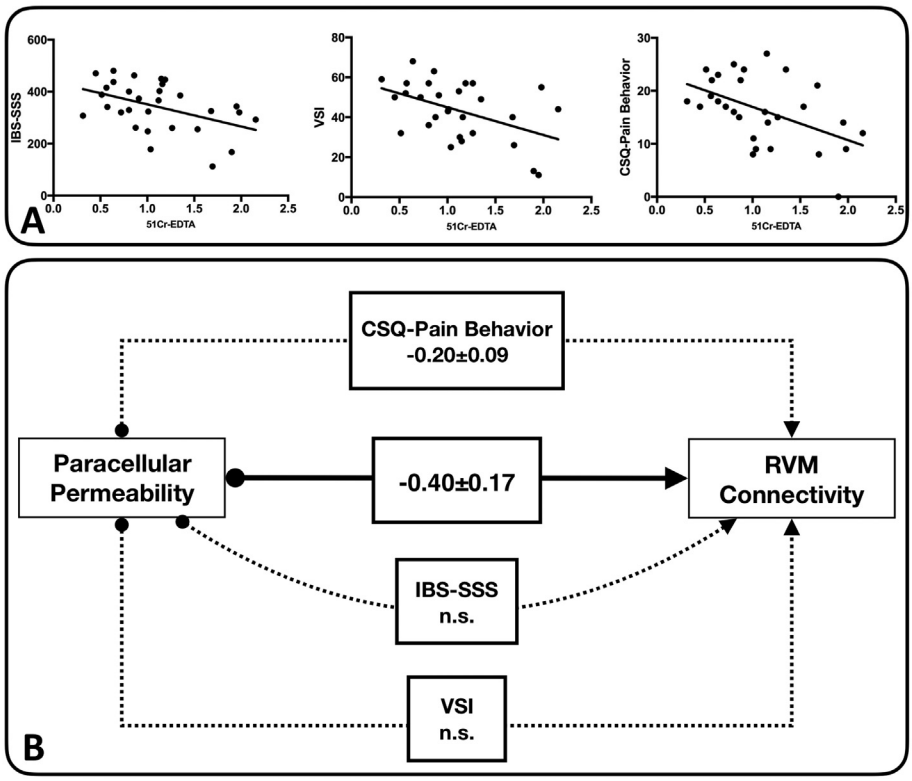

Fig. 6. Causality between gut and brain function in IBS. A. Graphs of those self-report questionnaires exhibiting significant correlations with levels of ^{51}Cr-EDTA passage in the IBS participants only. From left to right, these questionnaires were IBS-SSS, VSI, and the CSQ-Pain Behavior subscale. **B.** Causal path model used to assess the mediating effects of the three questionnaires shown in **A** on the effect of permeability on resting state functional connectivity in the RVM for the IBS patients only. Solid arrows indicate direct effects; dashed arrows indicate indirect effects. Significant and trend-level ($p < 0.01$) coefficients are shown in standardized form.

suggesting that IBS participants with elevated paracellular permeability may exhibit low-grade immune activation (Bednarska et al., 2017). For the IBS participants with more normal levels of paracellular permeability and absence of immune activation in the gut, the brain may not engage this endogenous pain inhibition system, and pain facilitatory mechanisms may dominate, as previously described (Mayer and Tillisch, 2011). For paracellular permeability, the path analysis results further indicate that in addition to a strong bottom-up component, there may be an additional top-down mechanism related to the use of adaptive versus maladaptive coping skills.

4.3. Limitations

The current study has a number of limitations. Firstly, the study sample size was small, making it difficult to fully elucidate the roles of either transcellular or paracellular permeability as a potential variable in IBS pathophysiology. Secondly, it was cross-sectional, such that only limited conclusions about causality can be made concerning the respective roles of transcellular and paracellular permeability and the brain in IBS symptom generation. As the study subjects reported moderate to severe symptoms, the findings need to be replicated in subjects with mild symptoms. Thirdly, due to the small sample size, we were unable to consider the role of menstrual cycle may have on both the measured brain features and their relationships with colonic permeability. At least one study has shown that DMN connectivity can change throughout the hormonal cycle (Petersen et al., 2014), however, a second study examining the relationship between pain perception and the menstrual cycle found no association (Vincent et al., 2011). Future studies should, in a larger sample, examine the role that the menstrual cycle may have on these results. Fourthly, as described in the Methods, the RS-fMRI data were acquired in an eyes-closed state, so care should be taken in comparing these results with those acquired in an eyes-open state. Similarly, we cannot guarantee that all participants were in a stable wakeful state during the entire RS-fMRI scan, so, as is unavoidable in most RS-fMRI scans (Tagliazucchi and Laufs, 2014), the results presented here may be contaminated with periods of sleep. Finally, the relationship between the brain and permeability is a bidirectional process involving top-down and bottom-up mechanisms, including autonomic nervous system modulation of permeability, which the current study was not designed to explore. Future studies should look at the etiology of the increased permeability in one of the IBS subgroups, and to confirm the hypothesis that mucosal immune activation is associated with increased permeability in this group.

5. Conclusions

The results from this study support the existence of structural and functional alterations in brain networks in female IBS participants, which are associated with changes in both paracellular and transcellular permeability. These associations between functional and structural brain features and gut permeability were significantly altered in IBS compared with the age-matched cohort of healthy women. The findings further suggest the potential existence of IBS subgroups, which differ in the way the brain and the gut interact. These differential brain responses may explain the inconsistency in previous reports about correlations of increased permeability with IBS symptoms and may have implications for differential treatment responses targeted at peripheral mechanisms.

Author contributions

S.T.W. was involved in data collection, data analysis, and interpretation and drafting of the manuscript. O.B. performed the sigmoidoscopies and was involved in study design, data acquisition, data analysis, and interpretation and drafting of the manuscript. A.V.K. was involved in data analysis, study design, and interpretation and drafting of the manuscript. A.I. was involved in data analysis and interpretation and drafting of the manuscript. M.P.J. was involved in data analysis and interpretation and drafting of the manuscript. S.E. was involved in interpretation and drafting of the manuscript. J.D.S. acquired funding, was involved in the interpretation of results, and assisted in editing the manuscript. M.E. was involved in interpretation and drafting of the

manuscript. E.A.M. was involved in study design and interpretation and drafting of the manuscript. S.W. performed the sigmoidoscopies and acquired funding, was involved in study design, and interpretation and drafting of the manuscript. All authors read the manuscript for critical content and approved the final version of the manuscript.

Conflicts of interest

The authors have declared that no conflicts of interest exist.

Acknowledgments

The authors wish to acknowledge the following funding sources: AFA FÖrskning (SW; AFA140417), Bengt-Ihre Fonden, County Council of Östergötland (SW; SLS-693541, SLS-503411), Region Östergötland (SW; LIO-700871, LIO-606201, LIO-536281, LIO-514271), and Deutsche Forschungsgemeinschaft (AI; DFG IC 81/1-1).

Appendix A. Supplementary data

Supplementary data to this article can be found online at https://doi.org/10.1016/j.nicl.2018.11.012.

References

Ahluwalia, V., Wade, J.B., Heuman, D.M., Hammeke, T.A., Sanyal, A.J., Sterling, R.K., Stravitz, R.T., Luketic, V., Siddiqui, M.S., Puri, P., Fuchs, M., Lennon, M.J., Kraft, K.A., Gilles, H., White, M.B., Noble, N.A., Bajaj, J.S., 2014. Enhancement of functional connectivity, working memory and inhibitory control on multi-modal brain MR imaging with Rifaximin in Cirrhosis: implications for the gut-liver-brain axis. Metab. Brain Dis. 29, 1017–1025.

Al-Chaer, E.D., Kawasaki, M., Pasricha, P.J., 2000. A new model of chronic visceral hypersensitivity in adult rats induced by colon irritation during postnatal development. Gastroenterology 119, 1276–1285.

Allen, E.A., Erhardt, E.B., Damaraju, E., Gruner, W., Segall, J.M., Silva, R.F., Havlicek, M., Rachakonda, S., Fries, J., Kalyanam, R., Michael, A.M., Caprihan, A., Turner, J.A., Eichele, T., Adelsheim, S., Bryan, A.D., Bustillo, J., Clark, V.P., Feldstein Ewing, S.W., Filbey, F., Ford, C.C., Hutchison, K., Jung, R.E., Kiehl, K.A., Kodituwakku, P., Komesu, Y.M., Mayer, A.R., Pearlson, G.D., Phillips, J.P., Sadek, J.R., Stevens, M., Teuscher, U., Thoma, R.J., Calhoun, V.D., 2011. A baseline for the multivariate comparison of resting-state networks. Front. Syst. Neurosci. 5, 2.

Andersson, J., Smith, S., Jenkinson, M., 2008. FNIRT-FMRIB's non-linear image registration tool. Hum. Brain Mapp. 2008.

Babo-Rebelo, M., Richter, C.G., Tallon-Baudry, C., 2016. Neural responses to heartbeats in the default network encode the self in spontaneous thoughts. J. Neurosci. 36, 7829–7840.

Bar, K.J., de la Cruz, F., Schumann, A., Koehler, S., Sauer, H., Critchley, H., Wagner, G., 2016. Functional connectivity and network analysis of midbrain and brainstem nuclei. NeuroImage 134, 53–63.

Bednarska, O., Walter, S.A., Casado-Bedmar, M., Strom, M., Salvo-Romero, E., Vicario, M., Mayer, E.A., Keita, A.V., 2017. Vasoactive intestinal polypeptide and mast cells regulate increased passage of colonic bacteria in patients with irritable bowel syndrome. Gastroenterology 153 (4), 948–960.e3.

Behbehani, M.M., 1995. Functional characteristics of the midbrain periaqueductal gray. Prog. Neurobiol. 46, 575–605.

Bell, A.J., Sejnowski, T.J., 1995. An information-maximization approach to blind separation and blind deconvolution. Neural Comput. 7, 1129–1159.

Berman, S.M., Naliboff, B.D., Suyenobu, B., Labus, J.S., Stains, J., Ohning, G., Kilpatrick, L., Bueller, J.A., Ruby, K., Jarcho, J., Mayer, E.A., 2008. Reduced brainstem inhibition during anticipated pelvic visceral pain correlates with enhanced brain response to the visceral stimulus in women with irritable bowel syndrome. J. Neurosci. 28, 349–359.

Bianciardi, M., Toschi, N., Edlow, B.L., Eichner, C., Setsompop, K., Polimeni, J.R., Brown, E.N., Kinney, H.C., Rosen, B.R., Wald, L.L., 2015. Toward an in vivo neuroimaging template of human brainstem nuclei of the ascending arousal, autonomic, and motor systems. Brain Connect 5, 597–607.

Bushnell, M.C., Ceko, M., Low, L.A., 2013. Cognitive and emotional control of pain and its disruption in chronic pain. Nat. Rev. Neurosci. 14, 502–511.

Calhoun, V.D., Adali, T., Pearlson, G.D., Pekar, J.J., 2001. A method for making group inferences from functional MRI data using independent component analysis. Hum. Brain Mapp. 14, 140–151.

Cryan, J.F., Dinan, T.G., 2012. Mind-altering microorganisms: the impact of the gut microbiota on brain and behaviour. Nat. Rev. Neurosci. 13, 701–712.

van den Heuvel, M., Mandl, R., Luigjes, J., Hulshoff Pol, H., 2008. Microstructural organization of the cingulum tract and the level of default mode functional connectivity. J. Neurosci. 28, 10844–10851.

Dinan, T.G., Cryan, J.F., 2013. Melancholic microbes: a link between gut microbiota and depression? Neurogastroenterol. Motil. 25, 713–719.

Drossman, D.A., Chang, L., 2016. Rome IV Multidimensional Clinical Profile (MDCP) for Functional Gastrointestinal Disorders, 1st ed. Rome Foundation.

Erhardt, E.B., Rachakonda, S., Bedrick, E.J., Allen, E.A., Adali, T., Calhoun, V.D., 2011. Comparison of multi-subject ICA methods for analysis of fMRI data. Hum. Brain Mapp. 32, 2075–2095.

Fairhurst, M., Wiech, K., Dunckley, P., Tracey, I., 2007. Anticipatory brainstem activity predicts neural processing of pain in humans. Pain 128, 101–110.

Francis, C.Y., Morris, J., Whorwell, P.J., 1997. The irritable bowel severity scoring system: a simple method of monitoring irritable bowel syndrome and its progress. Aliment. Pharmacol. Ther. 11, 395–402.

Freire, L., Mangin, J.F., 2001. Motion correction algorithms may create spurious brain activations in the absence of subject motion. NeuroImage 14, 709–722.

Freire, L., Roche, A., Mangin, J.F., 2002. What is the best similarity measure for motion correction in fMRI time series? IEEE Trans. Med. Imaging 21, 470–484.

Gebhart, G.F., 2004. Descending modulation of pain. Neurosci. Biobehav. Rev. 27, 729–737.

Gold, M.S., Gebhart, G.F., 2010. Nociceptor sensitization in pain pathogenesis. Nat. Med. 16, 1248–1257.

Grass, G.M., Sweetana, S.A., 1988. In vitro measurement of gastrointestinal tissue permeability using a new diffusion cell. Pharm. Res. 5, 372–376.

Grenham, S., Clarke, G., Cryan, J.F., Dinan, T.G., 2011. Brain-gut-microbe communication in health and disease. Front. Physiol. 2, 94.

Greve, D.N., Fischl, B., 2009. Accurate and robust brain image alignment using boundary-based registration. NeuroImage 48, 63–72.

Hall, G.B., Kamath, M.V., Collins, S., Ganguli, S., Spaziani, R., Miranda, K.L., Bayati, A., Bienenstock, J., 2010. Heightened central affective response to visceral sensations of pain and discomfort in IBS. Neurogastroenterol. Motil. 22, 276–280.

Himberg, J., Hyvarinen, A., Esposito, F., 2004. Validating the independent components of neuroimaging time series via clustering and visualization. NeuroImage 22, 1214–1222.

Hong, J.Y., Naliboff, B., Labus, J.S., Gupta, A., Kilpatrick, L.A., Ashe-McNalley, C., Stains, J., Heendeniya, N., Smith, S.R., Tillisch, K., Mayer, E.A., 2016. Altered brain responses in subjects with irritable bowel syndrome during cued and uncued pain expectation. Neurogastroenterol. Motil. 28, 127–138.

Jalbrzikowski, M., Larsen, B., Hallquist, M.N., Foran, W., Calabro, F., Luna, B., 2017. Development of white matter microstructure and intrinsic functional connectivity between the amygdala and ventromedial prefrontal cortex: associations with anxiety and depression. Biol. Psychiatry 82, 511–521.

Jenkinson, M., Smith, S., 2001. A global optimisation method for robust affine registration of brain images. Med. Image Anal. 5, 143–156.

Jenkinson, M., Bannister, P., Brady, M., Smith, S., 2002. Improved optimization for the robust and accurate linear registration and motion correction of brain images. NeuroImage 17, 825–841.

Jenkinson, M., Beckmann, C.F., Behrens, T.E., Woolrich, M.W., Smith, S.M., 2012. Fsl. NeuroImage 62, 782–790.

Keita, A.V., Gullberg, E., Ericson, A.C., Salim, S.Y., Wallon, C., Kald, A., Artursson, P., Soderholm, J.D., 2006. Characterization of antigen and bacterial transport in the follicle-associated epithelium of human ileum. Lab. Investig. 86, 504–516.

Kelly, J.R., Kennedy, P.J., Cryan, J.F., Dinan, T.G., Clarke, G., Hyland, N.P., 2015. Breaking down the barriers: the gut microbiome, intestinal permeability and stress-related psychiatric disorders. Front. Cell. Neurosci. 9, 392.

Kroenke, K., Spitzer, R.L., Williams, J.B., 2002. The PHQ-15: validity of a new measure for evaluating the severity of somatic symptoms. Psychosom. Med. 64, 258–266.

Labus, J.S., Bolus, R., Chang, L., Wiklund, I., Naesdal, J., Mayer, E.A., Naliboff, B.D., 2004. The Visceral Sensitivity Index: development and validation of a gastrointestinal symptom-specific anxiety scale. Aliment. Pharmacol. Ther. 20, 89–97.

Li, Y.O., Adali, T., Calhoun, V.D., 2007. Estimating the number of independent components for functional magnetic resonance imaging data. Hum. Brain Mapp. 28, 1251–1266.

Liu, X., Silverman, A., Kern, M., Ward, B.D., Li, S.J., Shaker, R., Sood, M.R., 2016. Excessive coupling of the salience network with intrinsic neurocognitive brain networks during rectal distension in adolescents with irritable bowel syndrome: a preliminary report. Neurogastroenterol. Motil. 28, 43–53.

Mahmood, A., Fitzgerald, A.J., Marchbank, T., Ntatsaki, E., Murray, D., Ghosh, S., Playford, R.J., 2007. Zinc carnosine, a health food supplement that stabilises small bowel integrity and stimulates gut repair processes. Gut 56, 168–175.

Mayer, E.A., Tillisch, K., 2011. The brain-gut axis in abdominal pain syndromes. Annu. Rev. Med. 62, 381–396.

Mayer, E.A., Naliboff, B.D., Craig, A.D., 2006. Neuroimaging of the brain-gut axis: from basic understanding to treatment of functional GI disorders. Gastroenterology 131, 1925–1942.

Mayer, E.A., Labus, J.S., Tillisch, K., Cole, S.W., Baldi, P., 2015a. Towards a systems view of IBS. Nat. Rev. Gastroenterol. Hepatol. 12, 592–605.

Mayer, E.A., Tillisch, K., Gupta, A., 2015b. Gut/brain axis and the microbiota. J. Clin. Invest. 125, 926–938.

Millan, M.J., 2002. Descending control of pain. Prog. Neurobiol. 66, 355–474.

Mulak, A., Bonaz, B., 2015. Brain-gut-microbiota axis in Parkinson's disease. World J. Gastroenterol. 21, 10609–10620.

Naliboff, B.D., Derbyshire, S.W., Munakata, J., Berman, S., Mandelkern, M., Chang, L., Mayer, E.A., 2001. Cerebral activation in patients with irritable bowel syndrome and control subjects during rectosigmoid stimulation. Psychosom. Med. 63, 365–375.

Napadow, V., Dhond, R., Park, K., Kim, J., Makris, N., Kwong, K.K., Harris, R.E., Purdon, P.L., Kettner, N., Hui, K.K., 2009. Time-variant fMRI activity in the brainstem and higher structures in response to acupuncture. NeuroImage 47, 289–301.

Neugebauer, V., 2015. Amygdala pain mechanisms. Handb. Exp. Pharmacol. 227, 261–284.

Neugebauer, V., Galhardo, V., Maione, S., Mackey, S.C., 2009. Forebrain pain mechanisms. Brain Res. Rev. 60, 226–242.
Ossipov, M.H., Morimura, K., Porreca, F., 2014. Descending pain modulation and chronification of pain. Curr. Opin. Support Palliat. Care 8, 143–151.
Petersen, N., Kilpatrick, L.A., Goharzad, A., Cahill, L., 2014. Oral contraceptive pill use and menstrual cycle phase are associated with altered resting state functional connectivity. NeuroImage 90, 24–32.
Pinto-Sanchez, M.I., Hall, G.B., Ghajar, K., Nardelli, A., Bolino, C., Lau, J.T., Martin, F.P., Cominetti, O., Welsh, C., Rieder, A., Traynor, J., Gregory, C., De Palma, G., Pigrau, M., Ford, A.C., Macri, J., Berger, B., Bergonzelli, G., Surette, M.G., Collins, S.M., Moayyedi, P., Bercik, P., 2017. Probiotic bifidobacterium longum NCC3001 reduces depression scores and alters brain activity: a pilot study in patients with irritable bowel syndrome. Gastroenterology 153, 448–459 e448.
Qin, C., Greenwood-Van Meerveld, B., Foreman, R.D., 2003a. Spinal neuronal responses to urinary bladder stimulation in rats with corticosterone or aldosterone onto the amygdala. J. Neurophysiol. 90, 2180–2189.
Qin, C., Greenwood-Van Meerveld, B., Foreman, R.D., 2003b. Visceromotor and spinal neuronal responses to colorectal distension in rats with aldosterone onto the amygdala. J. Neurophysiol. 90, 2–11.
Qin, C., Greenwood-Van Meerveld, B., Myers, D.A., Foreman, R.D., 2003c. Corticosterone acts directly at the amygdala to alter spinal neuronal activity in response to colorectal distension. J. Neurophysiol. 89, 1343–1352.
Rhee, S.H., Pothoulakis, C., Mayer, E.A., 2009. Principles and clinical implications of the brain-gut-enteric microbiota axis. Nat. Rev. Gastroenterol. Hepatol. 6, 306–314.
Rosenstiel, A.K., Keefe, F.J., 1983. The use of coping strategies in chronic low back pain patients: relationship to patient characteristics and current adjustment. Pain 17, 33–44.
Sandkuhler, J., 1996. The organization and function of endogenous antinociceptive systems. Prog. Neurobiol. 50, 49–81.
Smith, S.M., Nichols, T.E., 2009. Threshold-free cluster enhancement: addressing problems of smoothing, threshold dependence and localisation in cluster inference. NeuroImage 44, 83–98.
Smith, S.M., Jenkinson, M., Woolrich, M.W., Beckmann, C.F., Behrens, T.E., Johansen-Berg, H., Bannister, P.R., De Luca, M., Drobnjak, I., Flitney, D.E., Niazy, R.K., Saunders, J., Vickers, J., Zhang, Y., De Stefano, N., Brady, J.M., Matthews, P.M., 2004. Advances in functional and structural MR image analysis and implementation as FSL. NeuroImage 23, S208–S219 Suppl 1.
Smith, S.M., Johansen-Berg, H., Jenkinson, M., Rueckert, D., Nichols, T.E., Miller, K.L., Robson, M.D., Jones, D.K., Klein, J.C., Bartsch, A.J., Behrens, T.E., 2007. Acquisition and voxelwise analysis of multi-subject diffusion data with tract-based spatial statistics. Nat. Protoc. 2, 499–503.
Smith, S.M., Fox, P.T., Miller, K.L., Glahn, D.C., Fox, P.M., MacKay, C.E., Filippini, N., Watkins, K.E., Toro, R., Laird, A.R., Beckmann, C.F., 2009. Correspondence of the brain's functional architecture during activation and rest. Proc. Natl. Acad. Sci. U. S. A. 106, 13040–13045.
Son, Y.D., Cho, Z.H., Kim, H.K., Choi, E.J., Lee, S.Y., Chi, J.G., Park, C.W., Kim, Y.B., 2012. Glucose metabolism of the midline nuclei raphe in the brainstem observed by PET-MRI fusion imaging. NeuroImage 59, 1094–1097.
Son, Y.D., Cho, Z.H., Choi, E.J., Kim, J.H., Kim, H.K., Lee, S.Y., Chi, J.G., Park, C.W., Kim, J.H., Kim, Y.B., 2014. Individually differentiated serotonergic raphe nuclei measured with brain PET/MR imaging. Radiology 272, 541–548.
Stamford, J.A., 1995. Descending control of pain. Br. J. Anaesth. 75, 217–227.
Tagliazucchi, E., Laufs, H., 2014. Decoding wakefulness levels from typical fMRI resting-state data reveals reliable drifts between wakefulness and sleep. Neuron 82, 695–708.
Tillisch, K., Mayer, E.A., Labus, J.S., 2011. Quantitative meta-analysis identifies brain regions activated during rectal distension in irritable bowel syndrome. Gastroenterology 140, 91–100.
Tillisch, K., Labus, J., Kilpatrick, L., Jiang, Z., Stains, J., Ebrat, B., Guyonnet, D., Legrain-Raspaud, S., Trotin, B., Naliboff, B., Mayer, E.A., 2013. Consumption of fermented milk product with probiotic modulates brain activity. Gastroenterology 144, 1394–1401.e4.
Tracey, I., Bushnell, M.C., 2009. How neuroimaging studies have challenged us to rethink: is chronic pain a disease? J. Pain 10, 1113–1120.
Veinante, P., Yalcin, I., Barrot, M., 2013. The amygdala between sensation and affect: a role in pain. J. Mol. Psychiatry 1, 9.
Vincent, K., Warnaby, C., Stagg, C.J., Moore, J., Kennedy, S., Tracey, I., 2011. Dysmenorrhoea is associated with central changes in otherwise healthy women. Pain 152, 1966–1975.
van Wijck, K., Verlinden, T.J., van Eijk, H.M., Dekker, J., Buurman, W.A., Dejong, C.H., Lenaerts, K., 2013. Novel multi-sugar assay for site-specific gastrointestinal permeability analysis: a randomized controlled crossover trial. Clin. Nutr. 32, 245–251.
Winkler, A.M., Ridgway, G.R., Webster, M.A., Smith, S.M., Nichols, T.E., 2014. Permutation inference for the general linear model. NeuroImage 92, 381–397.
Woolrich, M.W., Jbabdi, S., Patenaude, B., Chappell, M., Makni, S., Behrens, T., Beckmann, C., Jenkinson, M., Smith, S.M., 2009. Bayesian analysis of neuroimaging data in FSL. NeuroImage 45, S173–S186.
Zhou, Q., Verne, M.L., Fields, J.Z., Lefante, J.J., Basra, S., Salameh, H., Verne, G.N., 2018. Randomised placebo-controlled trial of dietary glutamine supplements for post-infectious irritable bowel syndrome. Gut. https://doi.org/10.1136/gutjnl-2017-315136. (Published Online First: 14 August).
Zigmond, A.S., Snaith, R.P., 1983. The hospital anxiety and depression scale. Acta Psychiatr. Scand. 67, 361–370.